Inorg. Chem. **2007**, *46*, 231–237

Two Organically Templated Niobium and Zinconiobium Fluorophosphates: Low Temperature Hydrothermal Syntheses of $NbOF(PO_4)_2(C_2H_{10}N_2)_2$ and $Zn_3(NbOF)(PO_4)_4(C_2H_{10}N_2)_2$

Guang-Zhen Liu, Shou-Tian Zheng, and Guo-Yu Yang*

State Key Laboratory of Structural Chemistry, Fujian Institute of Research on the Structure of Matter, Chinese Academy of Sciences, Fuzhou, Fujian 350002, China

Received September 15, 2006

Two new niobium and zinconiobium fluorophosphates, $NbOF(PO_4)_2(C_2H_{10}N_2)_2$ (**1**) and $Zn_3(NbOF)(PO_4)_4(C_2H_{10}N_2)_2$ (**2**), have been prepared under hydrothermal conditions using ethylenediamine as a template. The structures were determined by single crystal diffraction to be triclinic, space group $P\bar{1}$ (No. 2), $a = 8.1075$ (6) Å, $b = 9.8961$ (7) Å, $c = 10.1420(8)$ Å, $\alpha = 111.655(1)°$, $\beta = 111.51(1)°$, $\gamma = 93.206(1)°$, $V = 686.19(9)$ Å^3, and $Z = 2$ for **1** and orthorhombic, space group *Fddd* (No. 70), $a = 9.1928(2)$ Å, $b = 14.2090(10)$ Å, $c = 32.2971$ (6) Å, $V = 4218.66(12)$ Å^3, and $Z = 8$ for **2**, respectively. Compound **1** is an infinite linear chain consisting of corner-sharing $[Nb_2P_2]$ 4-MRs bridged at the Nb centers with organic amines situated between chains, and compound **2**, containing the chains similar to that in **1**, forms a zeotype framework with organic amines situated in the gismondine-type $[4^68^4]$ cavities. The topology of **2** was previously unknown with vertex symbol 4·4·4·4·8·8 (vertex 1), $4\cdot4\cdot4\cdot8_2\cdot8\cdot8$ (vertex 2), $4\cdot4\cdot8\cdot8\cdot8_2\cdot8_2$ (vertex 3), and $4\cdot4\cdot4\cdot8_2\cdot8\cdot8$ (vertex 4). The topological relationships between the 4-connected network of **2** and several reported (3,4)-connected networks were discussed.

Introduction

Microporous materials are of great interest because of their rich structural chemistry and immense practical importance for commercial applications such as catalysis, absorption, separation, ion exchange, etc.[1−4] While mathematical possibilities are numerous for these materials, the number of topologies that can be realized in a chemical system is limited because of the restriction by the availability of basic chemical building units and their bonding requirements. The occurrence of microporous aluminophosphate[5] in the 1980s spurred widespread enthusiasm in the preparation of zeotype materials, other than initial aluminosilicates, with novel framework topologies or chemical compositions because the utility of these crystalline materials is intimately correlated to their geometrical features. To date, a very wide range of the transition metals (Sc, Ti, Zr, V, Cr, Mn, Fe, Co, Ni, Cu, Zn, Cd ect.) and main group elements (B, Al, Ga, In, etc.) have been incorporated into the frameworks of these solid-state materials, including phosphates and germanates.[6] Of particular interest is that incorporation of transition metal elements may lead to microporous materials with interesting electrical and magnetic properties.[7]

In contrast to well-characterized vanadium phosphate phases that display rich structural diversity, little research has been carried out on the synthesis of niobium phosphate analogues, which are usually prepared by solid-state reactions[8−15] or by high-temperature hydrothermal (≥600 °C)

* To whom correspondence should be addressed. E-mail: ygy@fjirsm.ac.cn. Fax: +86-591-8371-0051.

(1) Davis, M. E. *Chem. Mater.* **1992**, *4*, 756.
(2) Venuto, P. B. *Microporous Mater.* **1994**, *2*, 297.
(3) Barton, T. J.; Bull, L. M.; Klemperer, W. G.; Loy, D. A.; McEnaney, B.; Misono, M.; Monson, P. A.; Pez, G.; Scherer, G. W.; Vartuli, J. C.; Yaghi, O. M. *Chem. Mater.* **1999**, *11*, 2633.
(4) Davis, M. E. *Nature* **2002**, *417*, 813.
(5) Wilson, S. T.; Lok, B. M.; Messina, C. A.; Cannan, T. R.; Flanigen, E. M. *J. Am. Chem. Soc.* **1982**, *104*, 1146.
(6) Cheetham, K.; Férey, G.; Loiseau, T. *Angew. Chem., Int. Ed.* **1999**, *38*, 3268 and references therein.
(7) Cavellec, M.; Riou, D.; Férey, G. *Inorg. Chim. Acta* **1999**, *291*, 317.
(8) Levin, E. M.; Roth, R. S. *J. Solid State Chem.* **1970**, *2*, 250.
(9) Linde, S. A.; Gorbunova, Y. E.; Lavrov, A. V.; Tananaev, I. V. *Dokl. Akad. Nauk SSSR* **1980**, *250*, 96.
(10) Lavrov, V. *Izv. Akad. Nauk SSSR, Neorg. Mater.* **1982**, *18*, 996.
(11) Zid, M. F.; Jouini, T.; Jouini, N. *C. R. Acad. Sci. Paris, Ser. I.i* **1989**, *309*, 343.
(12) Leclaire, Borel, M. M.; Grandin, A.; Raveau, B. *J. Solid State Chem.* **1989**, *80*, 12.
(13) Raveau, Borel, M. M.; Leclaire, A.; Grandin, A. *Int. J. Modern Phys.* **1993**, *B7*, 4109.
(14) Leclaire, Borel, M. M.; Chardon, J.; Raveau, B. *J. Solid State Chem.* **1994**, *111*, 26.
(15) Fakhfakh, M.; Oyetola, S.; Jouini, N.; Verbaere, A.; Piffard, Y. *Mater. Res. Bull.* **1984**, *29*, 97.

10.1021/ic061752i CCC: $37.00
Published on Web 12/13/2006

reactions;[16,17] this can be attributed to the difference of chemical and physical characteristics between vanadium and niobium. First, vanadium may exhibit various oxidation states (from +3 to +5) and flexible coordination geometries (square pyramidal, octahedral, tetrahedral, and trigonal bipyramidal), whereas niobium usually exists with a valence of +5, exhibiting in an octahedral coordination geometry.[18,19] Second, the very low solubility of niobium source from typical commercial suppliers causes difficulties in the successful synthesis of niobium-containing materials with high crystallinity. It has been shown recently by Jacobson et al.[20] that crystalline niobium phosphates can be synthesized using low-temperature hydrothermal route, which is typically used for the synthesis of zeolite microporous materials. Furthermore, low-temperature hydrothermal reactions allow the use of organic structure-directing agents and enhance the possibilities for synthesizing new framework topologies. Unfortunately, so far, only one example of zeotype niobium-containing phosphates, $[(Nb_{0.9}V_{1.1})O_2(PO_4)_2(H_2PO_4)](N_2C_2H_{10})$, has been reported using organic amines as templates,[20d] the structure of which is closely similar to the vanadium phosphate analog $(VO)_2(PO_4)_2H_2PO_4 \cdot N_2C_2H_{10}$.[21]

Recently, we exploit a pathway to the formation of crystalline niobium phosphates with Nb_2O_5 as the niobium source at relatively low temperature by a two-step hydrothermal process. As a part of our ongoing research, herein we describe the syntheses, crystal structures, and thermal properties of two organically templated niobium and zinco-niobium fluorophosphates $NbOF(PO_4)_2(C_2H_{10}N_2)_2$ (**1**) and $Zn_3(NbOF)(PO_4)_4(C_2H_{10}N_2)_2$ (**2**) prepared hydrothermally using ethylenediamine as the template. Compound **1** is the first example of 1-D niobium phosphates templated by an organic amine consisting of corner-sharing $[Nb_2P_2]$ 4-MRs, and compound **2**, containing chain motifs similar to those found in **1**, form a 4-connected 3-D network with a new zeolite framework topology.

Experimental Section

Reagents. All reagents were of analytical grade and were used without further purification.

Synthesis. Compounds **1** and **2** were synthesized using a two-step hydrothermal technology in a 23 mL Teflon-lined autoclave. In a typical synthesis of compound **1**, 0.144 g of Nb_2O_5 was dissolved in 0.288 g of 48 wt % HF and heated to 110 °C for 24 h. After it was cooled, this solution was combined with 85% H_3PO_4 (0.15 mL), ethylenediamine (en, 0.3 mL), H_2O (4 mL), and ethylene glycol (3 mL) and heated at 180 °C for 7 days. Colorless rodlike crystals of **1** were recovered as the sole product of the reaction by filtration; they were washed with water and allowed to dry in air. The yield was greater than 95% based on Nb. Compound **2** was synthesized following the same procedure using 0.591 g of $Zn(H_2PO_4)\cdot 2H_2O$ as the starting material instead of H_3PO_4. The product, containing white polycrystalline powder and colorless prismlike single crystals in a yield of about 70% based on niobium, was separated by sonication and further washed by distilled water and then air-dried. IR (KBr, cm^{-1}): ν 3440s, 2917s, 2849s, 2728s, 2190m, 1642m, 1599m, 1553m, 1470w, 1355w, 1247w, 1098s, 1070s, 1021s, 982s, 914s, 880s, 799m, 635w, 587w, 554m, 539m, 489w, 452w for **1**; 3444s, 3220s, 2918s, 1621s, 1524s, 1458w, 1415w, 1381w, 1345w, 1328w, 1084s, 1053s, 1009s, 935s, 852s, 644s, 576s, 550s, 471m for **2**.

Analytical Procedures. Powder X-ray diffraction patterns (PXRD) were collected with a PANalytical X'Pert Pro diffractometer using Cu Kα radiation ($\lambda = 1.5418$ Å). Qualitative energy-dispersive spectroscopy (EDS) analyses of single crystals were performed on a JEOL JSM6700F field-emission scanning electron microscope equipped with a Oxford INCA system. Elemental analyses of C, H, and N were performed on an Elemental Vario EL III analyzer. Infrared spectra were recorded on an ABB Bomen MB 102 series FT-IR spectrophotometer at room temperature over the range of 4000−400 cm^{-1}, using a sample powder pelletized with KBr. The thermogravimetric analyses (TGA**)** were performed on a Mettler Toledo TGA/SDTA 851e analyzer. The samples were contained within alumina crucibles and heated at a rate of 10 °C min^{-1} from 30 to 900 °C in dry flowing N_2 (10 mL/min^{-1}).

Single-Crystal X-ray Studies. Crystals of **1** (dimensions 0.20 × 0.18 × 0.18 mm) and **2** (dimensions 0.40 × 0.28 × 0.20 mm) were selected for single-crystal analyses at room temperature. The data was collected using a Bruker Smart CCD diffractometer with graphite-monochromated Mo Kα radiation ($\lambda = 0.71073$ Å) over the range of $2.27° \le \theta \le 25.68°$ and $2.52° \le \theta \le 25.73°$ for compounds **1** and **2**, respectively. Of 3776 and 5180 reflections, 2575 and 970 were independent for compounds **1** and **2**, respectively. Absorption corrections were based on symmetry-equivalent reflections using the SADABS program.[22] The structures were solved by direct methods using the SHELXS program.[23] The heavy atoms (Nb, P, or Zn) were first revealed, and the remaining atoms (O, C, N) were placed from successive Fourier map analyses. In compound **1**, all the hydrogen atoms of the protonated ethylenediamine molecular were geometrically idealized and allowed to ride on their parent atoms; for compound **2**, the hydrogen atoms of the protonated ethylenediamine molecular were not totally fixed because it is disordered in two equivalent positions, and the corresponding carbon (C1) and nitrogen (N2) atoms have been refined with a 50% site occupancy factor. Oddly, a moderately large C−N (1.622 Å) distance is observed for the template molecule. This may reflect the motion of the organic molecule within the cavities of the structure. The refinements were performed using a full-matrix least-squares analysis with anisotropic thermal parameters for all non-hydrogen atoms. Crystallographic and refinement details are summarized in Table 1. The final R indices for **2** are moderately high probably because of the statistical disorder of organic amines and poor crystal quality.

(16) Longo, J. M.; Kierkegaard, P. *Acta Chem. Scand.* **1966**, *20*, 72.
(17) Liang, S.; Harrison, W. T. A.; Eddy, M. M.; Gier, T. E.; Stucky, G. *Chem. Mater.* **1993**, *5*, 917.
(18) Pope, M. T. *Heteropoly and Isopoly Oxometalates*; Springer: New Yark, 1983.
(19) Hagrman, P. J.; Finn, R. C.; Zubieta, *J. Solid State Sci.* **2001**, *3*, 745.
(20) (a) Wang, X.; Liu, L.; Cheng, H.; Jacobson, A. J. *Chem. Commun.* **1999**, 2531. (b) Wang, X.; Liu, L.; Jacobson, A. J. *J. Mater. Chem.* **2000**, *10*, 2774. (c) Wang, X.; Liu, L.; Cheng, H.; Ross, K.; Jacobson, A. J. *J. Mater. Chem.* **2000**, *10*, 1203. (d) Wang, X.; Liu, L.; Jacobson, A. J. *J. Mater. Chem.* **2002**, *12*, 1824. (e) Wang, X.; Liu, L.; Jacobson, A. J. *J. Solid State Chem.* **2004**, *177*, 194.
(21) Harrison, W. T. A.; Hsu, K.; Jacobson, A. J. *Chem. Mater.* **1995**, *7*, 2004.
(22) Sheldrick, G. M. *SADABS, A Program for the Siemens Area Detector Absorption Correction*; University of Göttingen: Göttingen, Germany. 1997.
(23) (a) Sheldrick, G. M. *SHELXS97, Program for Solution of Crystal Structure*; University of Göttingen: Göttingen, Germany, 1997. (b) Sheldrick, G. M. *SHELXS97, Program for Solution of Crystal Refinement*; University of Göttingen: Göttingen, Germany, 1997.

Table 1. Crystal and Structure Refinement Data for **1** and **2**

	1	**2**
empirical formula	$C_4H_{20}FN_4NbO_9P_2$	$C_4H_{20}FN_4NbO_{17}P_4Zn_3$
fw	442.09	828.25
space group	$P-1$	Fddd
a (Å)	8.1075(6)	9.1928(2)
b (Å)	9.8961(7)	14.2090(1)
c (Å)	10.1420(8)	32.2971(6)
α (deg)	111.655(1)	90
β (deg)	111.51(1)	90
γ (deg°)	93.206(1)	90
V (Å^3)	686.19(9)	4218.66(12)
Z	2	8
d_{calcd} (g cm^{-3})	2.140	2.608
μ(Mo Kα) (mm^{-1})	1.175	6.482
F(000)	448	3264
θ range (deg)	2.27−25.68	2.52−25.73
R1 [$I > 2\sigma(I)$][a]	0.0461	0.0798
wR2 [$I > 2\sigma(I)$][b]	0.1072	0.1708

[a] $R1 = \sum(|F_o| - |F_c|)/\sum|F_o|$. [b] $wR2 = \{\sum[w(|F_o|^2 - |F_c|^2)^2]/\sum[w(|F_o|^2)^2]\}^{1/2}$.

Results and Discussion

Synthesis and Chemical Composition. Single crystals of the compounds **1** and **2** were hydrothermally synthesized by following similar procedures in the presence of ethylenediamines as structure-directing agents. The incorporations of enH$_2$ (diprotontized ethylenediamine) in the compounds were confirmed by FT-IR spectra and subsequent single-crystal structure refinements. Hydrofluoric acid not only plays a key role of dissolving the starting reaction material Nb$_2$O$_5$ but also subsequently takes part in the structure constructions of the title compounds. The powder X-ray diffraction patterns of the bulk products are in good agreement with the calculated patterns based on the single crystal solutions (Figure 1), indicating the phase purity of the samples. Elemental analysis gives C, H, and N contents of 10.73, 4.38, and 12.61% (calcd C, 10.86; H, 4.52; N, 12.67%) for compound **1**, and 5.86, 2.58 and 6.84% (calcd C, 5.80; H, 2.42; N, 6.76%) for compound **2**, respectively. Energy dispersive spectroscopy (EDS) gives the Nb/P/F ratio as 1.0: 2.1:1.2 (calcd 1:2:1) for compound **1** and the Nb/Zn/P/F ratio as 1:2.9:4.2:1.3 (calcd 1:3:4:1) for compound **2**. These results are in agreement with their respective formulas found from the single crystal analyses.

Crystal Structures. The asymmetric unit of **1** (Figure 2) contains one crystallographically distinct Nb site and two unique P sites. The Nb atom is octahedrally coordinated, and the P atoms are all tetrahedrally coordinated. The four equatorial oxygen atoms of the Nb octahedron with Nb−O bond lengths of 1.987(4)−2.041(4) Å are shared by four phosphate tetrahedra; the two apical positions of the octahedron are completed by a short terminal Nb═O bond of 1.736(4) Å and a weak terminal Nb−F bond of 2.133(3) Å. Notably, the geometrical parameters of the distorted NbO$_5$F octahedron are very close to that of geometry-optimized [NbOF$_5$]$^{2-}$ (1.771 Å for Nb═O and 2.129 Å for *trans*-Nb−F)[24] and known niobium oxyfluorides.[24,25,26] Bond valences calculated[27] for the apical Nb═O and Nb−F bonds of the octahedron are 1.60 and 0.43 valence units, respectively. Similar lower values are commonly found in niobium oxyfluorides such as [NbOF(PO$_4$)](N$_2$C$_5$H$_7$) (1.25 for Nb═O, 0.74 for Nb−F)[20d] and [4-apyH]$_2$[Cu(4-apy)$_4$(NbOF$_5$)$_2$] (1.63 for Nb═O, 0.45 for *trans*-Nb−F),[25] suggesting that strong hydrogen bonds are formed between the guest cations and two terminal anions (see below). P(1) and P(2) each share two oxygen atoms with adjacent Nb atoms with P−O bond lengths in the range of 1.551−1.562 Å, leaving two terminal oxygen groups with shorter P═O bond lengths between 1.508 and 1.526 Å. The P−O and P═O bond lengths are in good agreement with those reported for similar compounds in the literature.[28,29]

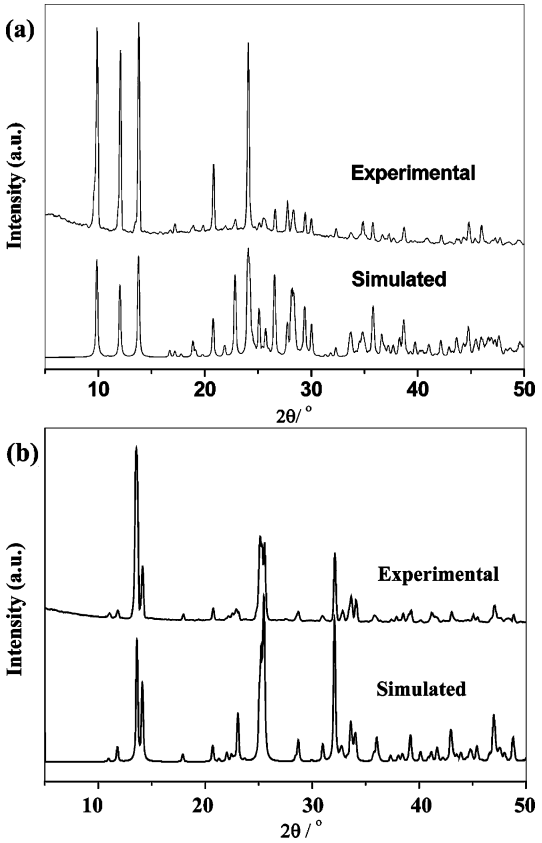

Figure 1. Simulated and experimental powder X-ray diffraction patterns of compounds **1** (a) and **2** (b).

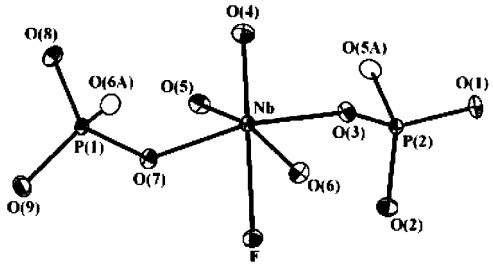

Figure 2. ORTEP plot of the asymmetric unit showing the local coordination environments of cations in compound **1**, with the symmetry-related part drawn as open circles. Thermal ellipsoids are given at 30% probability.

(24) Welk, M. E.; Norquist, A. J.; Arnold, F. P.; Stern, C. L.; Poeppelmeier, K. R. *Inorg. Chem.* **2002**, *41*, 5119.
(25) Izumi, H. K.; Kirsch, J. E.; Stern, C. L.; Poeppelmeier, K. R. *Inorg. Chem.* **2005**, *44*, 884.
(26) Heier, K. R.; Norquist, A. J.; Wilson, C. G.; Stern, C. L.; Poeppelmeier, K. R. *Inorg. Chem.* **1998**, *37*, 76 and references therein.
(27) Brown, I. D.; Altermatt, D. *Acta Crystallogr., Sect. B* **1985**, *41*, 244.
(28) Natarajan, S. *Inorg. Chem.* **2002**, *41*, 5530.

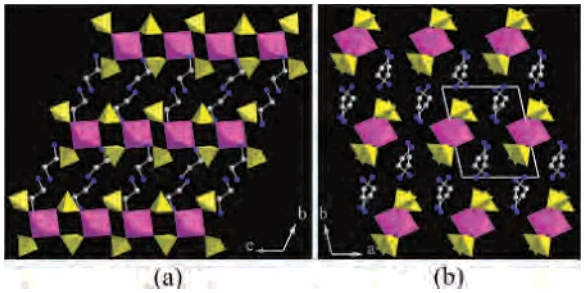

Figure 3. Views of the structure of **1** (a) along the [1 0 0] direction and (b) along the [0 0 1] direction: PO_4, yellow tetrahedra; NbO_5F, purple octahedra.

The inorganic host of **1** is an infinite anionic chain running along the [001] direction with corner-sharing $[Nb_2P_2]$ 4-MRs bridged at the Nb centers (Figure 3a). Sch a 1-D chain constructed by corner-sharing 4-MRs can be observed in several metal phosphates such as gallophosphates[29] and iron phosphates.[30] Similar chains totally based on tetrahedral metal sites are ubiquitous in the phosphate system[28,31−37] and can be found as the building bock in some layered or 3-D phosphates.[38−41] The chains of composition $NbOF(PO_4)_2^{2-}$ are separated by charge-balancing enH_2 cations. In the [001] projection, each inorganic chain is surrounded by six enH_2 stacks, in turn, each of which is surrounded by three inorganic chains (Figure 3b). There is extensive hydrogen bonding between the N atoms of enH_2 cations and O/F atoms in the inorganic chains with bond distances of N···O = 2.709(6)−3.157(6) Å and N···F = 2.736(6)−3.184(6) Å, respectively.

The asymmetric unit of **2** (Figure 4) contains one crystallographically distinct Nb atom that lies at a site with D_2 crystallographic symmetry, two distinct Zn atoms, of which Zn(1) also lies at a site with D_2 crystallographic symmetry and Zn(2) resides on the twofold symmetry axis, and a unique P atom in general position. The Nb atom is octahedrally coordinated, sharing four equatorial oxygen atoms with adjacent P atoms, with uniform Nb−O bond of 1.983(8) Å. The two apical corners of the octahedron are randomly occupied by terminal fluorine and oxygen atoms with a Nb−

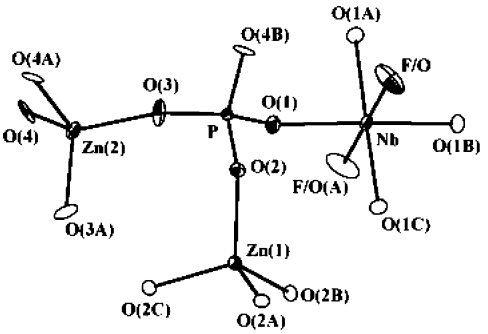

Figure 4. ORTEP plot of the asymmetric unit showing the local coordination environments of cations in compound **2**, with the symmetry-related part drawn as open circles. Thermal ellipsoids are given at 30% probability.

O/F bond length of 1.924(12) Å. The disordered terminal sites on NbO_5F octahedra are typical for niobium oxyfluorides,[20d,42,43] similar to the $[NbOF_5]^{2-}$ cases where the anions conform to the centricity of the crystal lattice.[25,26,44] These are also in accordance with the discussions on the distortion of the niobium octahedron (see below). The Zn and P atoms are tetrahedrally coordinated with the Zn−O bond lengths in the range of 1.935(9)−1.944(8) Å and the P−O bond distances between 1.506(9) and 1.571(10) Å. The average O−T−O angles are 109.7(4) and 109.1(7)° for ZnO_4 and PO_4, respectively, typical for tetrahedral geometries. Bond valence sums[27] for all unique atoms were calculated and are in good accordance with their formal oxidation states except for that of the disordered terminal anion on the niobium octahedron. The lower value calculated for the terminal atom (0.76 for F and 0.97 for O) seems to show that the anion is a hydroxyl; however, the Nb−O/F bond length of 1.924(12) Å is not uncommon in niobium phosphates containing similar disordered NbO_5F octahedra[20d,43] and niobium oxyfluorides containing $[NbOF_5]^{2-}$ anions.[24−26] In addition, energy-dispersive spectroscopy (EDS) shows that **2** contains the F atom. Therefore, the terminal atom was assigned as disordered O/F atom, not an OH group. Charge-balancing criterion confirmed that this assignment is reasonable.

There are only Nb−O−P and Zn−O−P linkages in the framework of **2**. The basis of the structure is an infinite linear chain along the [100] direction, which is similar to that in **1** except that one-half of the 4-connected Nb octahedra are substituted alternately by $Zn(1)O_4$ tetrahedra. The fully 4-connected 3-D network of **2** is completed by cross-linking between six $Zn(2)O_4$ tetrahedra stacks along the [100] direction and by connection of each infinite linear chain via sharing oxygen atoms (Figure 5). Each $Zn(2)O_4$ tetrahedra is corner-shared with four P tetrahedra from adjacent three corner-sharing chains, of which two are from the same chain and the other two are from different chains; such connections leads to new types of 1-D zigzag chains constructed by side-sharing 4-MRs. These side-sharing chains propagate parallel

(29) Walton, R. I.; Millange, F.; Bail, A. L.; Loiseau, T.; Serre, C.; O'Hare, D.; Férey, G. *Chem. Commun.* **2000**, 203.
(30) Cavellec, M.; Riou, D.; Greneèhe, J.; Férey, G. *Inorg. Chem.* **1997**, *36*, 2187.
(31) Loiseau, T.; Serpaggi, F.; Férey, G. *Chem. Commun.* **1997**, 1093.
(32) Rao, C. N. R.; Natarajan, S.; Neeraj, S. *J. Am. Chem. Soc.* **2000**, *122*, 2810.
(33) Chiang, R. *J. Solid State Chem.* **2000**, *153*, 180.
(34) Wang, K.; Yu, J.; Li, C.; Xu, R. *Inorg. Chem.* **2003**, *42*, 4597.
(35) Yu, J.; Sugiyama, K.; Hiraga, K.; Togashi, N.; Terasaki, O.; Tanaka, Y.; Nakata, S.; Qui, S.; Xu, R. *Chem. Mater.* **1998**, *10*, 3636.
(36) Huo, Q.; Xu, R.; Li, S.; Ma, Z.; Thomas, J. M.; Jomes, R. H.; Chippindale, A. M.; *Chem. Commun.* **1992**, 875.
(37) Chen, P.; Li, J.; Yu, J.; Wang, Y.; Pan, Q.; Xu, R. *J. Solid State Chem.* **2005**, *178*, 1929.
(38) Oliver, S.; Kuperman, A.; Ozin, G. A. *Angew. Chem., Int. Ed.* **1998**, *37*, 46.
(39) Yu, J.; Xu, R. *Acc. Chem. Res.* **2003**, *36*, 481.
(40) Jones, R. H.; Thomas, J. M.; Xu, R.; Huo, Q.; Xu, Y.; Cheetham, A. K.; Bieber, D. *Chem. Commun.* **1990**, 1170.
(41) (a) Williams, I. D.; Yu, J.; Gao, Q.; Chen, J.; Xu, R. *Chem. Commun.* **1997**, 1273. (b) Ayi, A. A.; Choudhury, A.; Natarajan, S. *J. Solid State Chem.* **2001**, *156*, 185. (c) Wang, K.; Yu, J.; Song, Y.; Xu, R. *Dalton Trans.* **2003**, 99. (d) Wei, B.; Yu, J.; Shi, Z.; Qiu, S.; Yan, W.; Terasaki, O. *Chem. Mater.* **2000**, *12*, 2065.
(42) Francis, R. J.; Jacobson, A. J. *Chem. Mater.* **2001**, *13*, 4676.
(43) Liu, G.-Z.; Zheng, S.-T.; Yang, G.-Y., *Chem. Commun.* **2006**, in press (DOI:10.1039/B614265F).
(44) Halasyamani, P. S.; Heier, K. R.; Norquist, A. J.; Stern, C. L.; Poeppelmeier, K. R. *Inorg. Chem.* **1998**, *37*, 369.

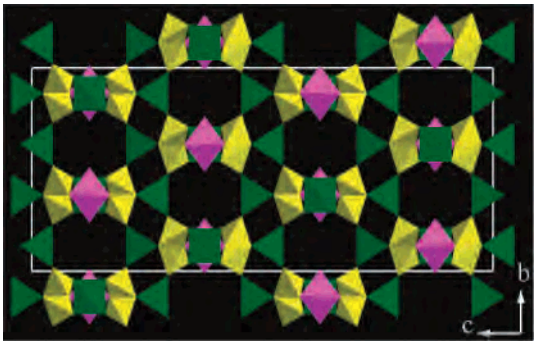

Figure 5. 3-D host framework of **2** viewed along the [1 0 0] direction: PO_4, yellow tetrahedra; ZnO_4, green tetrahedra; NbO_5F, purple octahedra.

to the crystallographic [1 1 0], [1 −1 0], [0 1 1] and [0 −1 1] directions and are cross-linked to the corner-sharing 4-MRs chains. According to the aufbau principle of building higher-D structures from that of the lower-D ones,[45] wherein the 0-D, especially 4-MRs, and the 1-D structures are considered to be synthons of the more complex structures. It is conceivable that the 3-D framework of **2** can be considered to result from the progressive reassembly of the 4-MRs or the resulting 1-D chain precursor observed in **1** through Zn^{2+} cations, considering their similar synthetic conditions. One of notable examples is an aluminophosphate $NiAlP_2O_8{\cdot}C_2N_2H_9$, assembled by a transformation mechanism of "chain-to-chain-3-D framework" so that the edge-sharing 4-MR chains first transform to the corner-sharing 4-MR chains and then assemble to 3-D open framework through Ni^{2+} cations.[34]

The resulting 3-D framework of **2** contains multidirectional interpenetrated channels that appear to have 4- and 8-MR openings. Figure 5 shows the 8-MR channels along the [1 0 0] direction. In addition, there are also other 8-MR channels along the [2 1 1], [2 −1 1], [2 1 −1], [−2 1 1], [1 1 0], and [−1 1 0] directions. Thus, **2** has a multidirectional pore system.

The network of **2** is closely related to that of the zeolite gismondine (GIS topology),[46] in that it possesses only 4- and 8-MRs and generates a 3-D channel system with gismondine-type [$4^6 8^4$] cavities (Figure 6a) at each channel intersection. The framework topology of zeolite gismondine can be simply considered as a periodic diamond-type array of the [$4^6 8^4$] cavities, in which the centers of the cavities sit on the nodes of diamond net ($6_2{\cdot}6_2{\cdot}6_2{\cdot}6_2{\cdot}6_2$),[47] whereas the network of **2** is a novel periodic array of the [$4^6 8^4$] cavities based on net ($6{\cdot}6{\cdot}6{\cdot}6_2{\cdot}6_2{\cdot}6_2$) (Figure 6b),[48] which is closely related to the diamond net and both nets can be readily intergrown. In fact, compound **2** has a previously unknown framework topology (Figure 7) with the vertex symbol $4{\cdot}4{\cdot}4{\cdot}4{\cdot}8{\cdot}8$ (vertex 1), $4{\cdot}4{\cdot}4{\cdot}8_2{\cdot}8{\cdot}8$ (vertex 2), $4{\cdot}4{\cdot}8{\cdot}8{\cdot}8_2{\cdot}8_2$ (vertex 3), and $4{\cdot}4{\cdot}4{\cdot}8_2{\cdot}8{\cdot}8$ (vertex 4). In addition, it is

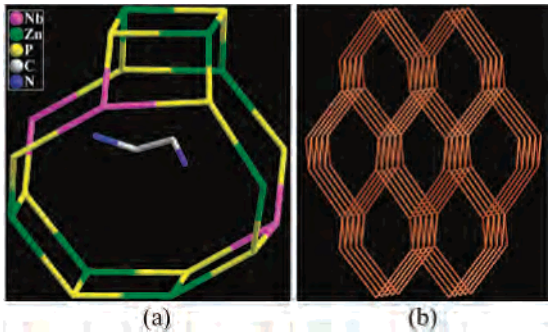

Figure 6. (a) [$4^6 8^4$] cage encapsulating an ethylenediamine in **2**. Oxygen atoms and the disordered parts of ethylenediamine are omitted for clarity. (b) Net ($6{\cdot}6{\cdot}6{\cdot}6_2{\cdot}6_2{\cdot}6_2$) of [$4^6 8^4$]] cage centers in **2** related to diamond net ($6_2{\cdot}6_2{\cdot}6_2{\cdot}6_2{\cdot}6_2$).

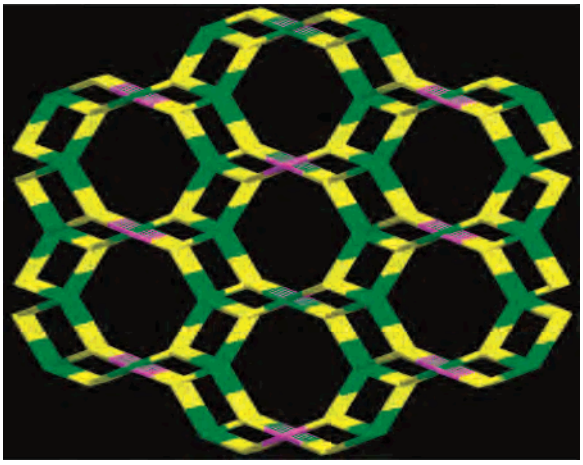

Figure 7. Framework topology of **2** along the [1 0 0] direction: P, yellow; Zn, green; Nb, purple.

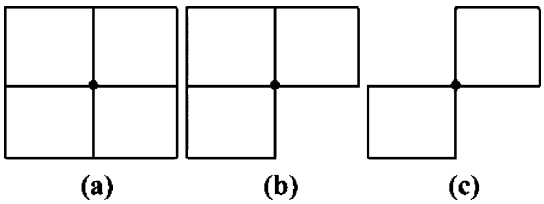

Figure 8. Three types of T-atom loop configurations observed in the **2** framework topology. The loop configuration is a simple graph showing how many 3- or 4-membered rings a given T-atom is involved in. In **2**, with four crystallographically unique T-atoms including two unique Zn atoms adopting the a and b configurations shown here, one unique P atom adopting the b type, and one unique Nb atom adopting the c type.

noticeable that three types of loop configurations (Figure 8) are found in the **2** framework topology, one of which (Figure 8a) is extremely rare in 4-connected structures and only occurs in the zeolite CZP framework type.[46] The new framework topology was predicted by Wiebcke;[47] he described a (3,4)-connected zincophosphate of [$Zn_3(HPO_4)_4$]-(NMe_4)$_2$ with interrupted **2** topology, which may be considered to be a **2** framework structure with local interruptions on the Nb sites to produce four terminal P−OH groups surrounding each vacant tetrahedral site. In other words, the (3,4)-connected network can be derived from the 4-connected network of **2** by removing one-eighth of all of the tetrahedral nodes. Other related cases are three examples of (3,4)-connected zincophosphites, templated by $(CH_3)_4N^+$, $(CH_3)_3NH^+$, and $(CH_3)_2NH_2^+$ respectively, with similar

(45) Rao, C. N. R.; Natarajan, S.; Choudhury, A.; Neeraj, S.; Ayi, A. A. *Acc. Chem. Res.* **2001**, *34*, 80.
(46) Baerlocher, C.; Meier, W. M.; Olson, D. H. *Atlas of Zeolite Framework Types*; Elsevier: Amsterdam, 2001; http://www.iza-structure.org/databases.
(47) Wiebcke, M. *J. Mater. Chem.* **2002**, *12*, 421.
(48) O'Keeffe, M.; Breese, N. E. *Acta Crystallogr., Sect A* **1992**, *48*, 663.

Table 2. Features of the $[NbOF_5]^{2-}$, $[NbO_5F]^{6-}$, and $[NbO_2F_4]^{3-}$ Octahedra in Particular Structures

			features of niobium octahedra				
compounds	types of octahedra	ref	Nb═O (Å)	*trans*-Nb−F (Å)	origin of distortion	direction of primary distortion	bridging atoms
$[4\text{-apyH}]_2[Cu(4\text{-apy})_4(NbOF_5)_2]$	$[NbOF_5]^{2-}$	25	1.730(3)	2.118(2)	SOJT[a]	apical O atom	apical O atom
$Cd(3\text{-apy})_4NbOF_5$	$[NbOF_5]^{2-}$	25	1.914(3)	1.937(3)	SOJT bond networks	apical O atom	apical O, F atom
$[HNC_6H_6OH]_2[Cu(py)_4(NbOF_5)_2]$	$[NbOF_5]^{2-}$	24	1.763(1)	2.098(1)	SOJT bond networks	apical O atom	apical O atom
$[pyH]_2[Cu(py)_4(NbOF_5)_2]$	$[NbOF_5]^{2-}$	55	1.728(8)	2.099(8)	SOJT bond networks	apical O atom	apical O atom
$Cu(3\text{-apy})_4NbOF_5$	$[NbOF_5]^{2-}$	25	1.919(1)	1.919(1)	none found	none found	apical O, F atom
$Na_{13}Nb_3P_6O_{28}F_2$	$[NbO_5F]^{6-}$	43	1.932(7)	1.932(7)	none found	none found	equatorial O atom
Compound **1**	$[NbO_5F]^{6-}$	this work	1.736(4)	2.133(3)	SOJT	apical O atom	equatorial O atom
Compound **2**	$[NbO_5F]^{6-}$	this work	1.924(12)	1.924(12)	none found	none found	equatorial O atom
$(C_2H_{10}N_2)_2[Nb_2O_3F_8]$	$[NbO_2F_4]^{3-}$	56	1.766/1.736	2.097/2.061	SOJT bond networks	side (O−O)	one of O atoms
			1.906/1.936	2.172/1.982			

[a] Second-order Jahn-Teller effects.

interrupted **2** topology.[49] In these structures, the distribution of four P−H groups adopts the tetrahedral pattern surrounding a vacant tetrahedral node. The centroid of these four phosphorus positions would correspond to the position of missing tetrahedral nodes.

Compared with the NMe_4^+ cation, which is well-known to direct the formation of small cavities,[50] the enH_2 cation encapsulated in the $[4^68^4]$ cavity of **2** is disordered because the special site of the molecule and because the hydrogen atoms could not be located. Despite this, it seems that hydrogen-bonding interactions exist between the enH_2 cation and the oxygen atoms of the framework through a plethora of short N···O separations between 2.823 and 3.248 Å.

Distortion of Niobium Octahedra. The out-of-center distortions for octahedrally coordinated early d^0 transition metals are very common and can be understood on the basis of the second-order Jahn-Teller effect (electronic effect).[51−53] Other secondary distortions, such as the bond-network effect, lattice stresses, and cation−cation repulsions, work together symbiotically to stabilize the distortions in mixed-metal oxides.[54]

However, in NbO_xF_{6-x} ($x = 1$ or 2) octahedra, only the filled p orbitals of the oxide ligands can mix with vacant cation d orbitals because the energy of the fluoride p orbitals is too low for any significant mixing to occur. The result is a spontaneous distortion of the central niobium cation toward each oxide ligand.[24] The primary distortion is inherent to the oxyfluoride anions and is not dependent on the extended crystal structure, and the direction of this distortion can be a corner ($x = 1$) or edge ($x = 2$) of the octahedron, depending on the number of oxide ligands.

For the $[NbOF_5]^{2-}$ anion, the primary distortion results in a short apical Nb═O bond and a long *trans*-Nb−F bond, and a secondary distortion can also be observed when bond-network interactions (including hydrogen bonding) around the anion occur asymmetrically.[24,25,55] For the NbO_5F octahedron in **1**, the shortening of the apical Nb−O bond and lengthening of the *trans*-Nb−F bond is similar to that for the $[NbOF_5]^{2-}$ anion; nevertheless, the approximately symmetrical bond networks about the octahedron causes symmetrical lengthening and shortening of bonds making detection of a secondary distortion impossible. Furthermore, it is notable that the crystallographic disorders in the apical positions can lead to the acentric $[NbOF_5]^{2-}$ anion and NbO_5F octahedron occupying a center of inversion in the crystal structures in the expense of its distortion, as shown in **2** and other similar niobium oxyfluorides.[20c,25] In addition, the unique *cis*-NbO_2F_4 octahedron is found in the dimer $(C_2H_{10}N_2)_2[Nb_2O_3F_8]$,[56] where the primary distortion results in a slight displacement of the niobium center cation toward an edge (O−O), and incidentally, bond-network effects modify the primary distortion. Table 2 shows a concise comparison of the $[NbOF_5]^{2-}$, $[NbO_5F]^{6-}$, and $[NbO_2F_4]^{3-}$ octahedral distortions based on the structures described here.

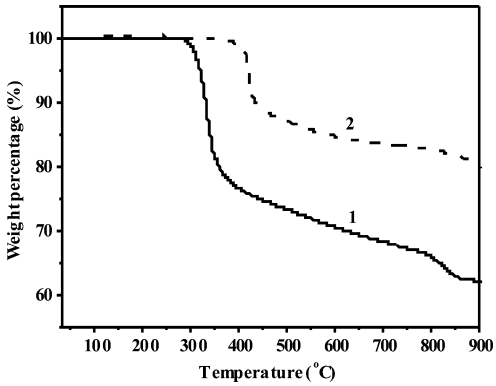

Figure 9. TGA curves of **1** and **2**.

Thermal Analysis. The thermal analysis (Figure 9) of **1** reveals a weight loss of 23.64% between 270 and 400 °C, followed by a further weight loss of 14.23% between 400 and 880 °C. The calculated total weight loss (37.83%),

(49) Chen, L.; Bu, X. *Inorg. Chem.* **2006**, *45*, 4654.
(50) Baerlocher, C.; Meier, W. M. *Helv. Chim. Acta* **1970**, *53*, 148.
(51) Burdett, J. K. *Molecular Shapes*; Wiley-Interscience: New York. 1980.
(52) Wheeler, R. A.; Whangbo, M. H.; Hughbanks, T.; Hoffmann, R.; Burdett, J. K.; Albright, T. A. *J. Am. Chem. Soc.* **1986**, *108*, 2222.
(53) Kang, S. K.; Tang, H.; Albright, T. A. *J. Am. Chem. Soc.* **1993**, *115*, 1971.
(54) Kunz, M.; Brown, I. D. *J. Solid State Chem.* **1995**, *115*, 395.
(55) Halasyamani, P.; Willis, M. J.; Stern, C. L.; Lundquist, P. M.; Wong, G. K.; Poeppelmeier, K. R. *Inorg. Chem.* **1996**, *35*, 1367.
(56) Nicholas, F. S.; Philip, L. *Acta Crystallogr., Sect. C* **2005**, *61*, m344.

corresponding to 1.5 H_2O (6.11%) and one HF (4.52%), as well as combustion of two ethylenediamine molecules (27.19%) per formula unit by assuming a residual composition of $1/2Nb_2O_5 \cdot P_2O_5$, is in agreement with the observed values. The TGA data for **2** shows that the compound is stable up to ~380 °C and subsequently decomposes to lose two ethylenediamines (14.51%), 1.5 H_2O (3.26%), and one HF (2.41%) per formula unit. The marked weight loss of 20.16% up to 900 °C agrees with the calculated value of 20.18% by assuming that the final product is mixture of $3ZnO \cdot {}^1/_2Nb_2O_5 \cdot 2P_2O_5$.

Conclusion

A two-step hydrothermal process was employed to synthesize two organically templated niobium and zinconiobium fluorophosphates using ethylenediamine as the template. The inorganic host of **1** is characterized by an infinite anionic chain consisting of corner-sharing 4-MRs, and the structure of **2** is based on infinite linear chains similar to that of **1**, except one-half of NbO_5F octahedra are substituted alternately by ZnO_4 tetrahedra, which are further cross-linked by additional ZnO_4 tetrahedra to produce a 4-connected 3-D network with a previously unknown framework topology. It is suggested that compound **1** may be thought of as a solid precursor to compound **2,** and we are investigating its possible transformation to other related niobium fluorophosphates, by the addition of other cations to further confirm the validity of our speculation. In addition, considering the large variety of organic templates that could be used in this synthetic regime, it is possible to isolate other open-framework niobium-based phosphates.

Acknowledgment. This work was supported by the NNSF of China (Nos. 20473093 and 20271050), the Talents Program of the Chinese Academy of Sciences, the NSF of Fujian Province (No. E0510030), and the State Important Scientific Research Program (No. 2006CB932904).

Supporting Information Available: Crystallographic information in CIF format for compounds **1** and **2**. This material is available free of charge via the Internet at http://pubs.acs.org.

IC061752I